Semi-automatic Segmentation of Multiple Sclerosis Lesion Based Active Contours Model and Variational Dirichlet Process'

Foued Derraz, Laurent Peyrodie, Antonio Pinti, Abdelmalik Taleb-Ahmed, Azzeddine Chikh, Patrick Hautecoeur

▶ **To cite this version:**

Foued Derraz, Laurent Peyrodie, Antonio Pinti, Abdelmalik Taleb-Ahmed, Azzeddine Chikh, et al.. Semi-automatic Segmentation of Multiple Sclerosis Lesion Based Active Contours Model and Variational Dirichlet Process'. Computer Modeling in Engineering and Sciences, 2010, 67 (2), pp.95-117. 10.3970/cmes.2010.067.095 . hal-00838375

HAL Id: hal-00838375
https://hal.science/hal-00838375

Submitted on 26 Jun 2013

HAL is a multi-disciplinary open access archive for the deposit and dissemination of scientific research documents, whether they are published or not. The documents may come from teaching and research institutions in France or abroad, or from public or private research centers.

L'archive ouverte pluridisciplinaire **HAL**, est destinée au dépôt et à la diffusion de documents scientifiques de niveau recherche, publiés ou non, émanant des établissements d'enseignement et de recherche français ou étrangers, des laboratoires publics ou privés.

Copyright © 2010 Tech Science Press CMES, vol.67, no.2, pp.95-116, 2010

Semi-automatic Segmentation of Multiple Sclerosis Lesion Based Active Contours Model and Variational Dirichlet Process

Foued Derraz[1], Laurent Peyrodie[2], Antonio PINTI[3], Abdelmalik Taleb-Ahmed[3], Azzeddine Chikh[4] and Patrick Hautecoeur[5]

Abstract: We propose a new semi-automatic segmentation based Active Contour Model and statistic prior knowledge of Multiple Sclerosis (MS) Lesions in Regions Of Interest (RIO) within brain Magnetic Resonance Images(MRI). Reliable segmentation of MS lesion is important for at least three types of practical applications: pharmaceutical trails, making decision for drug treatment, patient follow-up. Manual segmentation of the MS lesions in brain MRI by well qualified experts is usually preferred. However, manual segmentation is hard to reproduce and can be highly cost and time consuming in the presence of large volume of MRI data. In other hand, automated segmentation methods are significantly faster yielding reproducible results. However, these methods generally produced segmentation results that agree only partially with the ground truth segmentation provided by the expert. In this paper, we propose a new semi-automatic segmentation based Active Contour model for MS lesion that combines expert knowledge with a low computational cost to produce more reliable MS segmentation results. In particular, the user selects coarse RIO that encloses potential MS lesions and a sufficient background of the healthy White Matter tissues (WM). Having this two class statistic properties, we propose to extract texture features corresponding to health and MS lesion. The results draw showed a significant improvement of the proposed model.

Keywords: Multiple Sclerosis, Active Contours, Variational Dirichlet prior, Appearance priors, Level-set, Segmentation evaluation

[1] Faculté Libre de Médecine, F-59000 Lille, France
[2] Hautes Etudes d'Ingénieur, LAGIS (FRE CNRS 3303), 59650 Villeneuve d'ascq, France
[3] LAMIH (FRE CNRS 3304), Université de Valenciennes, F-59313 Valenciennes, France
[4] Genie Biomedical Lab,Abou Bekr Belkaid University, Tlemcen,13000, Algeria
[5] Groupe Hospitalier de l'Institut Catholique Lillois, Univ Nord de France, F-59000 Lille, France

1 Introduction

Image segmentation is one of the most important tasks in image processing and computer vision. In last two decades, image segmentation remains a challenging problem [Derraz, Beladgham, and Khelif (2004); Ma, Tavares, Jorge, and Mascarenhas (2010)], particularly because of the dependence of the problem on imaging modalities and on the imaged objects. In medical image processing, particularly as applied to magnetic resonance (MR) images of the brain, segmentation has drawn much attention during the past twenty years [Gonalves, Tavares, and Jorge (2008);Vasconcelos and Tavares (2008)]. The segmentation tasks in this area are aimed at classifying the component tissues of the brain such white matter gray matter, and at quantifying the volume and shape parameters of different brain tissues for serving in various neurological and neurosurgical applications such tumors extraction and Multiple Sclerosis (MS) detection [Filippi, Horsfield, and Ader (1998)].

Magnetic Resonance Imaging (MRI) is the most sensitive technique for detecting MS lesions [Kamber, Shinghal, Collins, Francis, and Evans (1995);Grossman and Mcgowan (1998)]. The change in lesion volume over time is often used as an objective measure of the evolution of the disease. Treatments have recently become available for MS, which may improve the long-term prognosis for patients [Benedict and Bobholz (2007)] and measuring the change in lesion load is likely to play an important part in many future phase clinical trials in MS as a secondary measure of outcome [Miller (2002)].

The most basic form of assessment involves manually tracing the outline of each MS lesion on each MRI brain slice to compute the total area and volume of lesions [Filippi, Horsfield, and Ader (1998)]. However, quantitative assessment of MS lesion is not without difficulty. This is due to their deformable shapes, their location across patients which can be significantly different; their intensity and texture characteristics may vary. The main issues are that many currently-employed image analysis methods are time consuming, and the volumes obtained are operator-dependent and prone to operator-induced errors [Bazin and Pham (2008); Khayati, Vafadust, Towhidkhah, and Nabav (2008)]. MS Lesions seen on MRI often have no clearly-defined borders, and the delineation of such borders is highly subjective. Many works have addressed the problem of improving the reproducibility of the measurement of MS lesion volumes using computer-assisted or automated segmentation methods for Brain MR image.

The Brain MR image segmentation strategies may be broadly classified into boundary-based, region-based, and hybrid strategies. Boundary-based approaches focus on delineating the interface between the object and the surrounding co-objects in the image. Region-based approaches, which are very prevalent in brain MR image

segmentation, focus on delineating the entire region occupied by the object in the image rather than its boundary [Ma, Tavares, Jorge, and Mascarenhas (2010); Wu, Warfield, Tan, Wells, Meier, van Schijndel, Barkhof, and Guttmann (2006) ;Gonalves, Tavares, and Jorge (2008)].

1.1 Related Works

Traditional methods commonly approach MS lesion segmentation problem by applying classification algorithms that rely on a pixel-by-pixel analysis, using primarily image intensities and knowledge issued from probabilitic or topological atlas [Bazin and Pham (2008);Shiee, Bazin, Ozturk, Reich, Calabresi, and Pham (2010)]. Neighborhood relations may be encoded through a Markov random field (MRF) model or other neighborhood statistics [Khayati, Vafadust, Towhidkhah, and Nabav (2008)]. However, we are unaware of an approach that uses regional statistical properties related to shape, boundaries and texture at different scales. A few automatic and semi-automatic segmentation methods have been designed specifically for MS detection.

A common approach for performing automatic lesion segmentation involves modeling the distribution of intensities in healthy brain MR images as a Gaussian Mixture Model (GMM) and then segmenting the lesions as outliers of this model. [Anbeek, Vincken, van Osch, Bisschops, and van der Grond (2004)] combined a K-Nearest Neighbor (KNN)classifier with an elastic template registration to segment the MS brains. In addition to intensity features provided by the input images, the classifier also used features from a distance map generated from a digital template. The method iterates between KNN classification and elastic registration of the digital template to the hard segmentation of the MS brain generated by the classifier to refine the segmentation of structures and lesions. A similar approach is introduced by [Wu, Warfield, Tan, Wells, Meier, van Schijndel, Barkhof, and Guttmann (2006)] where intensity-based KNN classification is followed by a template-driven segmentation and partial volume artifact correction technique to improve the classification. In another work [Warfield, Dengler, Zaers, Guttmann, Wells, Ettinger, Hiller, and Kikinis (1995)] used GMM to classify the major brain tissues and an elastically registered template is used to distinguish the healthy gray matter (GM) from (WM) combined with MS lesions. Lesions are then separated from (WM) using a minimum distance classifier.

In their work [Zijdenbos, Dawant, Margolin, and Palmer (2000)] developed an automatic segmentation method for T1-, T2-, and proton density (PD)-weighted images based on a supervised artificial neural network classifier and validated it extensively on multicenter clinical trial. [Zijdenbos, Forghani, and Evans (2000)] used a Gaussian mixture distribution and bias field correction to identify major brain tis-

sues and separate them from the lesions. [Van Leemput, Maes, V, Colchester, and Suetens (2001)] extended this framework by incorporating a probabilistic brain atlas along with neighborhood constraints.

[Ait-Ali, Prima, Hellier, Carsin, Edan, and Barillot (2005)]used an Enhanced Likelihood Estimator (ELE) to estimate a GMM from different time points. A Mahalanobis distance was used to distinguish the lesions from healthy tissue, and intensity constraints were imposed after this step to reduce the false positives. More recent methods further combined a ELE with a mean shift algorithm [GarciaLorenzo, Prima, Collins, Morrissey, and Barillot (2008)] or a Hidden Markov chain [Bricq, Collet, and Armspach (2008)]. [Souplet, Lebrun, Chanalet, and Ayache (2008)] used a TLE to segment the healthy tissue from T1 and T2 sequences, and derived a threshold from parameters of the healthy brain to delineate the lesions on an enhanced FLuid-Attennuated Inversion Recovery (FLAIR) sequence. These methods also segment lesions as outliers of the normal brain distribution. Instead of modeling lesions as outliers of a distribution, other methods model lesions as a separate class. [Harmouche, Collins, Arnold, Francis, and Arbel (2006)] introduced an unsupervised Bayesian lesion classifier with different intensity distributions for different regions of the brain. Lesions are segmented based on posterior probabilities and entropy values. [Freifeld, Greenspan, and Goldberger (2009)] used a constrained GMM to model the image and active contours to delineate lesions. Supervised classifiers that model lesions as distinct classes have also been used. [Nett (2001)] focused on Bayesian classifier. They improved the statistical classifier by non-parametric modeling of class conditional probabilities using parzen window and by a priori probabilities modeling of the class probabilities through a Markov random field (MRF) model. In addition, quantification was carried out by calculating the total volumes of normal and diseased (lesions) tissues.

[Wu, Warfield, Tan, Wells, Meier, van Schijndel, Barkhof, and Guttmann (2006)] tested three algorithms and proposed to combine template-driven segmentation, deformable anatomical atlas, and a heuristic connectivity-based Partial Volume Effect correction component, demonstrating the highest accuracy. [Wu, Warfield, Tan, Wells, Meier, van Schijndel, Barkhof, and Guttmann (2006)] expanded this method to a multi-channel MRI segmentation for detection of subtypes of MS lesions, improving sensitivity, specificity, and accuracy. [Souplet, Lebrun, Chanalet, and Ayache (2008)] perform automatic multi-stage segmentation for MS lesion from three MRI sequences (T1, T2 and T2-FLAIR). As a first step the images are normalized where the region of interest are focused. Secondly, a classification of the brain is performed based on expectation maximization algorithm [GarciaLorenzo, Prima, Collins, Morrissey, and Barillot (2008)] applied on the T1 and T2 sequences. In a third step, information given by the obtained segmentations and morphological

operations are used to extract lesions. [Admiraal-Behloul, van den Heuvel, Olofsen, van Osch, der Grond, van Buchem, and Reiber (2005)] used a grouping artificial immune network to segment the brain from T1 and T2 sequences, extracted CSF from the T1 image, and segmented the lesions on the T2 image with masked cerebro-spinal fluid (CSF).

Recently, a new approach is proposed for fully automatic segmentation of MS lesions in fluid attenuated inversion recovery (FLAIR) Magnetic Resonance (MR) images. The proposed approach, based on a Bayesian classifier, utilizes the Adaptive Mixtures Method (AMM) and Markov random field (MRF) model to obtain and upgrade the class conditional probability density function and the a priori probability of each class. [Shiee, Bazin, Ozturk, Reich, Calabresi, and Pham (2010)] proposed in their paper a fully automatic segmentation method based topological atlas. To compare the performance of the proposed approach with those of previous approaches including manual segmentation, the similarity criteria of different slices related to 14 MS patients were calculated. Also, volumetric comparison of lesions volume between the fully automated segmentation and the gold standard was performed using correlation coefficient. The results showed a better performance for the proposed approach, compared to those of previous works.

1.2 Our Contribution

This paper introduces a novel semi automatic segmentation method based on a combination of a powerful multiscale classification based a variational Dirichlet process and region based active contours model. By combining segmentation and classification, we are able to utilize integrative, regional properties that provide regional statistics, characterize their overall shapes, and localize their boundaries. Our method offers the following advantages. First, it relies on an variational segmentation method, multiscale classification approach to provide a hierarchical decomposition of a MRI scan in only linear time complexity. Second, we incorporate an novel rich set of multiscale features to guide the active contours segmentation and to characterize MS lesions. We further calculate a Bhattachryya distance to discriminate MS lesion. Third, our method is general and flexible, and can be adapted to handle other, similar medical problems. Fourth, similar to other approaches, the method is semi-automatic and can fully automatic due to the use of a probabilistic brain atlas. We further use atlas data to identify the cerebellum due to the difficulty in detection of MS in this area. Finally, our algorithm provides a soft classification result with different levels of MS disease probability rather than just a binary result. As the anticipated extent of the lesions may vary significantly between experts, this property can be valuable for clinical analysis.

The paper is organized as follows. In next section we introduces the segmentation

method, in section II presents the feature extraction method, and Section III describes the classification based Dirichlet Process in our segmentation method. In Section IV, experiments on two types of brain MRI data are presented. Section V follows with a discussion and conclusions.

2 Method

2.1 Segmentation method

MS lesions are not randomly distributed throughout the brain or white matter, but are known to occur more frequently in certain locations and have characteristic sizes [Filippi, H. van Waesberghe, A. Horsfield, Bressi, Gasperini, A. Yousry, L. Gawne-Cain, Morrissey, A. Rocca, Barkhof, J. Lycklama-Nijeholt, Bastianello, and H. Miller (1997)]. The pathological features of MS lesions vary widely, but the result is usually an increase in the water content, and of the tissue water within lesions [Johnston, Atkins, Mackiewich, and Anderson (1996)]. The incorporation of domain-specific prior information is therefore in three parts. The first relates to the known intensity characteristics of the image feature-in this case MS lesions-relative to the surrounding non-feature pixels. The second consists of a probabilistic model of the spatial variation in the size characteristics of the features. Finally, we incorporate a probabilistic model of the known spatial distribution of the feature. The probabilistic models for size and distribution of MS lesions were derived from a sample of 280 MRI scans from the MS patient population, with the lesions manually segmented by domain experts.

2.1.1 Intensity Hints

Often, the intensity distribution of image features relative to the background non-feature pixels is non-Gaussian, but well characterized. For example, on PD-weighted images, MS lesions are brighter than the background tissue and CSF, and very bright pixels adjacent to a seed pixel would always be considered part of the lesion, regardless of the brightness relative to the mean. Thus, an intensity hint allows the intensity distribution in the feature to be highly skewed, where our domain knowledge tells us that these pixels must be part of the feature.

2.1.2 Construction of the Prior Distributions

A sample of 14 MS patients was used as a representative selection from the population. All were scanned as part of other MRI-based studies using a double-echo pulse sequence, and all had given written informed consent for their scans to be used for research purposes. All scans were acquired with 0.94-mm in-plane resolution, 3-mm slice thickness, a 512x512 image matrix, and 521 slices covering the en-

tire brain. The patients were from three MS disease subtypes (primary-progressive, relapsing-remitting, and secondary progressive), with 6 woman patients and 8 man patient. The subgroups have different typical lesion volumes [Anbeek, Vincken, van Osch, Bisschops, and van der Grond (2004)] and possibly different spatial distributions. However, when we examined visually the spatial distribution for the subgroups individually, we found no discernible differences between them except for an intensity scaling because of the differences in mean lesion volume. Thus, it was decided to combine scans from all three subgroups to form a single template. In figure (1) we represent two slice from template images for MS patients,

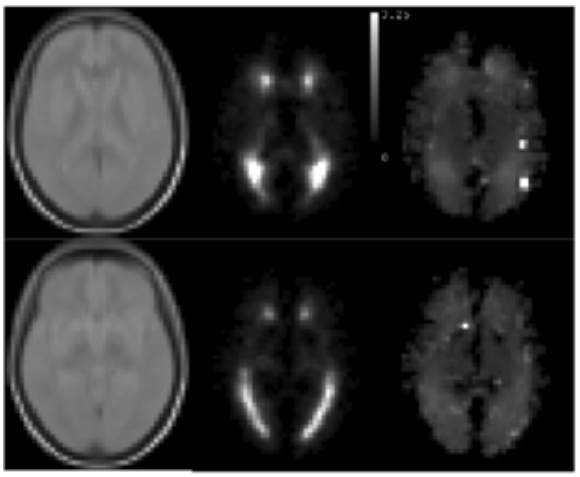

Figure 1: Two representative slices from the template images formed from 14 MS patients, from left to right, the T1 MR images are represented, the pre ventricular structure are represented and the extracted brain structure are represented

where the lesions have been outlined using the contouring method, on the left is the proton-density weighted template; center is the lesion probability; and on the right is the lesion feature size image. Intensity scale applies to the lesion probability images. Note the high frequency of occurrency of lesions in the periventricular areas, particularly around the horns of the lateral ventricles, a well-documented feature of typical MS lesions. Feature size image is noisy in locations where there are few lesions amongst the 14 patients at that location, and so the feature size estimate is based on only a few data The lesions on each scan were identified by a neurologist with neuroimaging expertise, and outlined by an experienced neurologist or technician, who delineated the borders as ROIs using the contouring method [He, Peng, Everding, Wang, Han, Weiss, and Wee (2008)]. Three sets of involved in the

segmentation of all patient subgroups. It is expected that any errors in segmentation would be averaged out over the large sample of 14 patients, unless such errors are systematic as could result, for example, if lesions in certain locations are less distinct and more difficult to delineate. In order to form the lesion size and probability maps, it was first necessary to register all images into a standard anatomical space. First, the PD images from all patients were averaged to form an initial target image.The target was then down-sampled from the original 512X512x512 pixels to 256x256x256 pixels. Next, each of the PD images was registered to the target image, and the registered images were averaged to form a new target image. This process was repeated five times, when no substantive changes were seen in the target after a further iteration. Registration was performed using the root mean square difference in intensity as the similarity measure to assess the difference between the target and registered images [Wells, Grimson, Kikinis, and Jolesz (1996)], and the types of deformation of the registered image allowed were rigid body (translation and rotation) and scaling in three orthogonal directions. Intensity rescaling was performed as part of the registration procedure so that all registered images contributed equally to the final average PD template image. Two representative slices from the resulting average PD template image are shown in in fig. 1. Using the lesion ROIs as a mask, binary images of the lesions were produced for each patient, which were then transformed to the coordinate space of the template image, using the same transform as was found when registering the PD image to the template. The transformed binary images were then summed, divided by the number of patients in the sample, and downsampled to 256x256x256 pixels, to give the probability (relative frequency) of lesion occurrence at each anatomical position. This downsampling provides additional spatial smoothing so that the lesion frequency map can be constructed using a smaller patient sample. Furthermore, any subsequent slight errors in registration to the template will have minimal impact because of the spatial smoothing

2.2 Active Contours Model based Statistical knowledge

The basic idea consists of finding a regular closed curve $\partial\Omega$ discriminating the image domainΩ_I into pair-wise disjoint regions. For an image $I:\Omega\subset R^2\rightarrow R^+$ defined on an open and bounded domain Ω. Binary segmentation consists of finding a regular closed curve $\partial\Omega$ partitioning the domain Ω into image partition. Image partitioning $P(\Omega)$ can be calculated by the Maximum A Posteriori (MAP) of partitioning probability $p(P(\Omega)|I)$. In Bayesian Framework partitioning probability can be expressed as:

$$p(P(\Omega)|I)\propto p(I|P(\Omega))\,p(P(\Omega)) \tag{1}$$

where image-based cues in the first term, represented as data likelihood and related to the region statistics is separated from second term corresponding to the geometric properties of the partition. The basic idea is to obtain the best $\partial\Omega$ by maximizing the conditional probability:

$$\partial\hat{\Omega} = \arg\max \left\{ \underbrace{\log\left(\frac{1}{p\left(P\left(\Omega\right)\right)}\right)}_{E_b(\partial\Omega)} + \beta \underbrace{\log\left(\frac{1}{p\left(I|P\left(\Omega\right)\right)}\right)}_{E_{image}(\Omega,I)} \right\} \tag{2}$$

In equation (2), the first term corresponds to the geometric properties of the partition $P\left(\Omega\right)$. [Chan and Vese (2001);Cremers, Schnorr, and Weickert (2001)] consider the geometric properties of the partition that which favour a short length of partition boundary:

$$p\left(P\left(\Omega\right)\right) = \mathrm{e}^{-\int\limits_{\partial\Omega} k_b(\mathbf{x},\partial\Omega)da(\mathbf{x})} \tag{3}$$

where $\partial\Omega$ is the contour curve and $k_b\left(\mathbf{x},\partial\Omega\right)$ is boundary descriptor. The second energy term on the right side allows integrating texture descriptor. Although several texture energies and shape energies have been proposed in [O. Michailovich and Tannenbaum (2007)], most of them need a weighting β factor to balance the two energy's functional in order to make both of them equally important to the segmentation. In Equation (2), the second term $p\left(I|P\left(\Omega\right)\right)$ gives easier model than the posterior distribution $p\left(P\left(\Omega\right)|I\right)$. The second the term in equation (2) allows introducing prior knowledge. For that we assume that image partitioning $P\left(\Omega\right)$ consider only two pairwise $\{\Omega_1,\Omega_2\}$ disjoint regions $\left(\Omega_1 \cap \Omega_2\right) = \phi$. This can be summarized as:

- all the probabilities of observing an image I when Ω_1,Ω_2 partitions are equally possible: $p\left(I|\left\{\Omega_1,\Omega_2\right\}\right) = Bat\left(\Omega_1,\Omega_2\right)$ where Bat is the Bhattacharyya matching function [O. Michailovich and Tannenbaum (2007)].

- the pixels within each region are independent:

  $$p\left(I|\,\Omega_i\right) = \prod_{x\in\Omega_i} p_i\left(\mathbf{x}\right) \quad i = 1,2$$

Then the a posteriori probability can be expressed as:

$$\mathrm{p}\left(\mathrm{P}\left(\Omega\right)|\,I\right) \propto Bat\left(\Omega_1,\Omega_2\right)\mathrm{e}^{-\int\limits_{\partial\Omega} k_b(\mathbf{x},\partial\Omega)da(\mathbf{x})} \tag{4}$$

The Maximization of the a Posteriori Probability (MAP) in equation (4) can be done by minimizing its log-likelihood. The corresponding energy to MAP in equation (4) is expressed as:

$$E(\partial\Omega,\Omega_1,\Omega_2)=\int\limits_{\partial\Omega}k_b(\mathbf{x},\partial\Omega)\,da(\mathbf{x})+\beta\log\left(\frac{1}{Bat(\Omega_1,\Omega_2)}\right) \tag{5}$$

This also can be written using descriptor formulation as:

$$E(\partial\Omega,\Omega_1,\Omega_2)=\underbrace{\int\limits_{\partial\Omega}k_b(\mathbf{x},\partial\Omega)\,da(\mathbf{x})}_{E_b(\partial\Omega)}+\beta\underbrace{\int\limits_{\Omega}k_r(\mathbf{x},\Omega)\,d\mathbf{x}}_{E_{Image}(I,\Omega)} \tag{6}$$

Also, the region descriptor can be defined as Bhattacharyya distance [Rauber, Braun, and Berns (2008)]between two the probability densities defined as:

$$E(\partial\Omega,\Omega_1,\Omega_2)=\underbrace{\int\limits_{\partial\Omega}k_b(\mathbf{x},\partial\Omega)\,da(\mathbf{x})}_{E_b(\partial\Omega)}+\beta E_{image}(I,\Omega) \tag{7}$$

Where the statistical energy can be expressed as: $E_{image}(I,\Omega)=\log\left(\frac{1}{Bat(\Omega_1,\Omega_2)}\right)$ where is the Bhattacharyya coefficient given by [Rauber, Braun, and Berns (2008); O. Michailovich and Tannenbaum (2007)]:

$$Bat(\Omega_1,\Omega_2)=p(I|\{\Omega_1,\Omega_2\})=\sqrt{\int\limits_{\Omega}p(I|\Omega_1)\,p(I|\Omega_2)\,d\mathbf{x}} \tag{8}$$

The minimization of such energy functional can be efficiently implemented using the level set framework. Gaussians Mixture Model (GMM) represents straightforward uniform regions but fail to properly represent more complicated region statistics [Kim, III, Yezzi, Çetin, and Willsky (2005)]. We therefore estimate density by Parzen kernel, which can better describe the regions. This method estimates the PDF based on the histograms, using a smoothed Gaussian kernel:

$$p(I,\Omega_i)=\frac{1}{|\Omega_i|}\int\limits_{\Omega_i}k_\sigma(I-I(\Omega_i))\,d\mathbf{x} \tag{9}$$

where k_σ denote the Gaussian kernel. Others authors proposed to employ Kullback-Leibler [**?**] and claims that this distance give better resultants comparing to the

maximum likelihood. The minimization of such energy functional can be efficiently implemented using the level set framework. In the level set framework representation, a contour is the zero level set of an embedding function $\phi : \Omega \subset R^2 \rightarrow R$,$C(t) = \{\underline{x} \in \Omega | \phi(\underline{x}) = 0\}$. The energy functional in Equation (4) can now be expressed in level set framework as:

$$E(\phi) = \int_{\Omega} |\nabla H(\phi)| d\mathbf{x} + \beta \sqrt{\int_{\Omega} p(I|\Omega_1)\, p(I|\Omega_2)\, d\mathbf{x}} \tag{10}$$

The corresponding Euler-Lagrange evolution equation for ϕ is given by:

$$\frac{\partial \phi}{\partial t} = \delta(\phi) \left(div\left(\frac{\nabla \phi}{|\nabla \phi|}\right) - \beta \mathbf{V}_{Bat} \right) \tag{11}$$

where $H(\phi)$and $\delta(\phi) = \frac{dH(\phi)}{d\phi}$ respectively are the regularized Heaviside and Dirac delta functions respectively. In order to produce two regions, the MS lesion region Ω_1 and the brain tissues Ω_2, with two pdfs as disjoint as possible, the energy the functional is maximized, w.r.t the evolving domain Ω , is done with the shape derivative tool [S. Jehan-Besson (2003)]. Thus, the Eulerian derivative of $E_{image}(I,\Omega)$ in the direction ξ is as follows:

$$\left\langle \frac{\partial E_{image}(I,\Omega)}{\partial t}, \xi \right\rangle = \int_{\partial\Omega} V_{Bat} \left\langle \xi, \overrightarrow{N}(s) \right\rangle ds \tag{12}$$

where the Bhattacharyya velocity is expressed as:

$$\begin{aligned} \mathbf{V}_{Bat} = {} & \frac{1}{2}\left(\frac{1}{|\Omega_1|} - \frac{1}{|\Omega_2|}\right) \sqrt{p(I,\Omega_1)\, p(I,\Omega_2)} \\ & + \tfrac{1}{2}\left(\tfrac{1}{|\Omega_2|}\right) \int_{R^+} \sqrt{\tfrac{p(I,\Omega_1)}{p(I,\Omega_2)}} \left(k_\sigma(I - I(\Omega)) - \sqrt{p(I,\Omega_2)}\right) \\ & - \tfrac{1}{2}\left(\tfrac{1}{|\Omega_1|}\right) \int_{R^+} \sqrt{\tfrac{p(I,\Omega_2)}{p(I,\Omega_1)}} \left(k_\sigma(I - I(\Omega)) - \sqrt{p(I,\Omega_1)}\right) \end{aligned} \tag{13}$$

3 Region statistics in a multi-dimensional feature space

The Probability Density Functions (PDF) chosen to represent $p(I|\Omega_1)$, $p(I|\Omega_2)$ should:

- Capture the distribution of values in the region.
- Discriminate between the two regions.

MRI data usually has more than one modality (T1, T2, PD, FLAIR, T1-Gado). In addition, for analyzing the texture information in the MRI images we extract a set of features that better capture the image local scale and frequency. We therefore need to generalize the above formulation to vector valued data. Let $\chi = \{I_1, I_2, ..., I_m\}$ be the set of feature images. If we assume the features to be independent of each other [Bouguila and Ziou (2004);], the total a posteriori probability of the region $\Omega_i, (i = 1, 2)$ is:

$$p(\chi|\Omega_i) = \prod_{j=1}^{m} p\left(I_j\middle|\Omega_i\right) = \prod_{j=1}^{m} \prod_{\mathbf{x}\in\Omega_i} p_{i,j}(\mathbf{x}) \tag{14}$$

The independence hypothesis might not be valid in the case of significant correlation among features. In such a case the set features can be considered as multivariate data, where each pixel location corresponds to a dimensional vector [Bouguila and Ziou (2007)]. But estimating high dimensional nonparametric densities are high computational cost. We propose a clustering approach to handle the multivariate image data. The clustering features, was previously proposed by [Bouguila and Ziou (2006)], to identify texture patterns in a feature space but in the context of normalized cuts segmentation. Clustering has been proven to be a very effective method in image segmentation. Among them K-mean, spectral clustering, and probabilistic models [Bouguila and Ziou (2004);Bouguila (2008)] have been proposed and have been used often. One common problem with many of the clustering algorithms is that they are often parametric, in other words they find a pre-specified number of clusters. [Kurihara, Welling, and Vlassis (2006);Kurihara, Welling, and Teh (2007)] proposed a simple nonparametric probabilistic algorithm based on Dirichlet Processes (DP). Despite the simplicity since it uses a Gibbs sampling approach we feel that can be a slow algorithm to be applied in many image analysis area.

Most active contours based segmentation methods are used in an unsupervised setting where the region statistics are refined as the curve evolves [He, Peng, Everding, Wang, Han, Weiss, and Wee (2008)]. This might be quite effective if the region statistics are discriminative enough. But, as mentioned earlier, one of the main problems in MS segmentation is that the appearance of MS and surrounding tissue are not always obviously separated (not even in the feature space). We therefore have to use additional prior information to help the segmentation. The MS doesn't have a particular shape prior. In addition, the surrounding tissues such as the ventricles can be deformed and therefore don't preserve a shape prior. We therefore chose to use a prior on the appearance that better disambiguate the two regions. We used manually labeled data for getting an initial statistics for tumour/brain regions in the clustered feature space. More and ventricles when part of the ventricles are

incorrectly segmented as MS. We designed a prior that penalizes the clusters predominant in the ventricles from having a high probability in the MS. Hence, we assumed appearance priors for (p_1, p_2) skewed in such a manner that those prominent clusters in ventricles have a very low prior probability and the rest of the clusters have uniform probability. We used images with manually segmented MS and ventricles to identify the overlapping clusters. Given $D = \left[\widehat{I}^{(1)}, \widehat{I}^{(2)}, ..., \widehat{I}^{(N)}\right]$ a set of training cluster images. We denote θ the probability of cluster K and regard $\theta = \{\theta_1, \theta_2, ..., \theta_K\}$ as parameters of a Bayesian system.
Following the Dirichlet distribution, the posterior probability of a cluster is:

$$\begin{aligned} &p_i\left(\widehat{I}(x) = k \middle| D\right) = \int p_i\left(\widehat{I}(x) = k \middle| D, \theta\right) p(\theta|D)\, d\theta \\ &= \int \theta_k p(\theta|D)\, d\theta = E_{p(\theta|D)}[\theta_k] \end{aligned} \tag{15}$$

The posterior of $p(\theta)$ is again following a Dirichlet distribution, we get:

$$p_i\left(\widehat{I}(x) = k \middle| D\right) = E_{p(\theta|D)}[\theta_k] = \frac{\alpha_k + M_k}{\sum\limits_k \alpha_k + \sum\limits_k M_k} \tag{16}$$

where M_K's are the counts of the clusters in the training data. We can observe that by choosing a relatively low value for α_k, we can suppress the posterior probability of the cluster k. The posteriors (p_1, p_2) give the MS lesion, WM, GM, CSF probabilities in equation (6):

Preprocessing (1) Preprocessing and feature extraction (2) Clustering features (3) Compute WM probability prior and PDF of MS lesion , noted p_1 and p_2 Segmentation:

4 Evaluation of Segmentation results

Numerous evaluation segmentation methods are presented in literature [D. Martin (2004)].The performance the segmentation results were quantitatively compared against the "gold standard" using four different similarity measures :

$$F(P, R) = \frac{2PR}{P + R} \tag{17}$$

F-measure (F), percentage of correct estimation (P), percentage of over estimation R. The four similarity measures are formally defined as: where P precision descriptor measures segmentation precision, defined as:

$$P = \frac{\#(S \cap M)}{\#(S)} \tag{18}$$

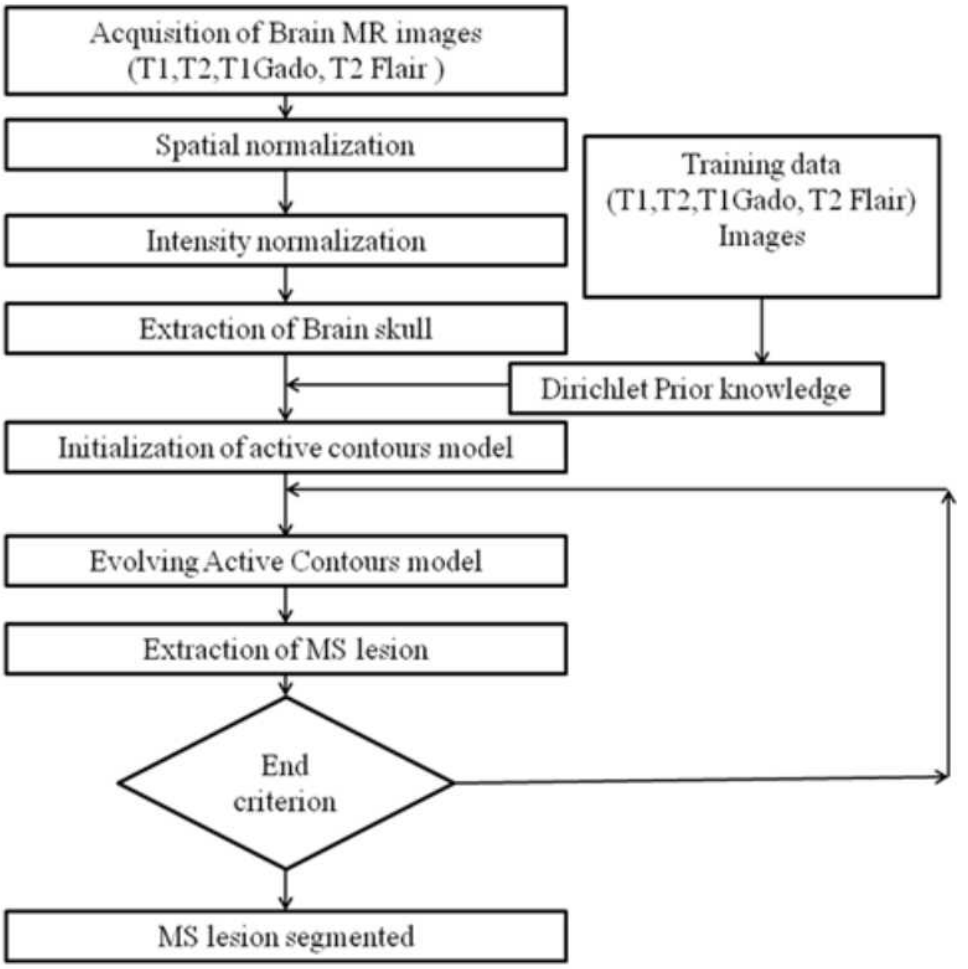

Figure 2: Our method flow chart and the different steep for MS lesion segmentation

And *R*as a recall descriptor measuring the consistency of the reference segmentation, defined as:

$$R = \frac{\#(S \cap M)}{\#(M)} \tag{19}$$

and are the numbers of pixels of contours respectively for segmented surface and the reference surface . indicates the number of pixels belonging to segmented contours and reference contours (segmentation realized by expert). As well as assessing the reproducibility of the lesion volumes, we also required to evaluate the

degree to which the lesion pixels determined on each analysis corresponded spatially.
If the lesion surface correspond to a high degree, but are determined using a different set of pixels, then other factors must be at work when an observer determines the lesion surface. If an observer delineates a set of pixels , on a scan on one occasion and a different set of pixels , on a second evaluation, then we define the concordance between the two measures as:

$$Concordance = \frac{\#(S \cap M)}{\#(S \cup M)} \tag{20}$$

When exactly the same sets of pixels are delineated on both occasions, the concordance will be 100; when there is no overlap of the pixels delineated, the concordance will be zero. In order to assess the concordance on the scan-rescan evaluations, it is, of course, first necessary to spatially register the two scans in order that the pixel locations correspond anatomically. The registration was performed using the root mean square difference in intensity as the similarity measure [citederraz05], and allowing a rigid-body transform (translation and rotation).
The same transform was applied to a binary lesion image produced by using the lesion ROIs as a mask, with linear interpolation. The resulting transformed lesion image was, however, blurred by the interpolation process and it was necessary to threshold this transformed image to produce a new binary lesion image. The threshold level was set so that the lesion volume in the transformed image was the same as the volume in the original untransformed binary image. The degree of concordance was then assessed using (15).

5 Experiments results

5.0.1 MRI Scanning

A total of 14 definite MS patients, including 8 female and six male with average age of 40 years old, were selected in this study according to the revised Mc Donald criteria 2005 [Wu, Warfield, Tan, Wells, Meier, van Schijndel, Barkhof, and Guttmann (2006)]. Mean disease duration for the patients was five years. For all patients the same MR images were obtained via a GE 1.5T scanner. All images were acquired according to full field MRI criteria of MS in T2-w, T1-weighted (T1-w), Gadolinium enhanced T1-weighted, and FLAIR in axial, sagittal and coronal surfaces. We selected the FLAIR images, especially axial ones, with lesions in deep, priventricular, subcortical, and cortical white matters (supratentorial lesions). More lesion load and higher accuracy of FLAIR in revealing of these MS lesions were the reason for this selection. Also, FLAIR is especially helpful for pri-ventricular lesions closely opposed to an ependymal surface, where they may be obscured by the high

signal CSF on T2-w images. Scan parameters of, repetition time (TR)/echo time (TE)/inversion time (TI), for FLAIR images were 9000/144/2500 ms, TR/TE for T1-w images were 424/10 ms and TR/TE for T2-w images were 3820/105 ms. Each image volume consisted of averagely 40 slices.

As a preprocessing step, the images first had to be scaled. Therefore the range between zero intensity and maximum intensity, M, in the original 12-b data (I) was scaled to a new intensity (IS) between 0 and 255 (8-bit) which is obtained by: IS =I/M*255.

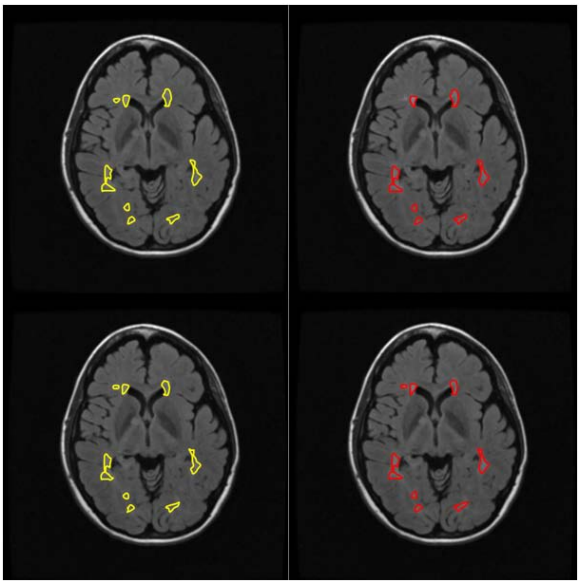

Figure 3: Example segmentations using the active contour model; Left column shows segmentations lesions are outlined in yellow. Left column shows segmentations using manual contouring that are broadly similar, but differ in detail

Table 1: Quantitative evaluation of the segmentation

Method	Our method	Navee method	Khyati method	Van Lempt Method
Error	8%	8%	12%	13,2%
P	80%	80%	75%	65%
R	80%	80%	75%	65%
Concordance	79%	79%	72%	68%

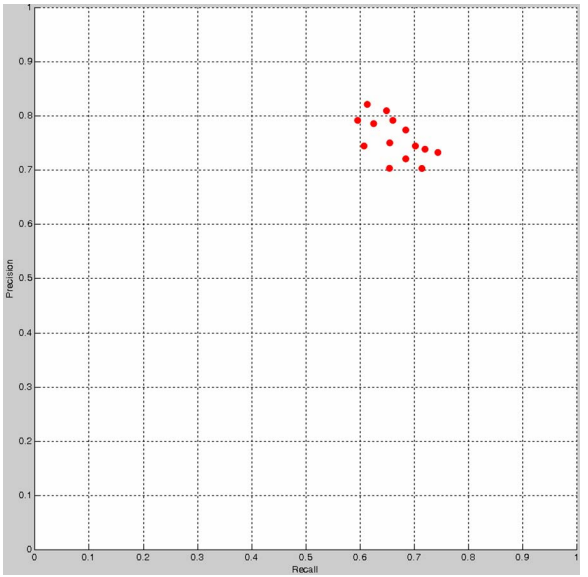

Figure 4: Precision of our method in term of F-measure

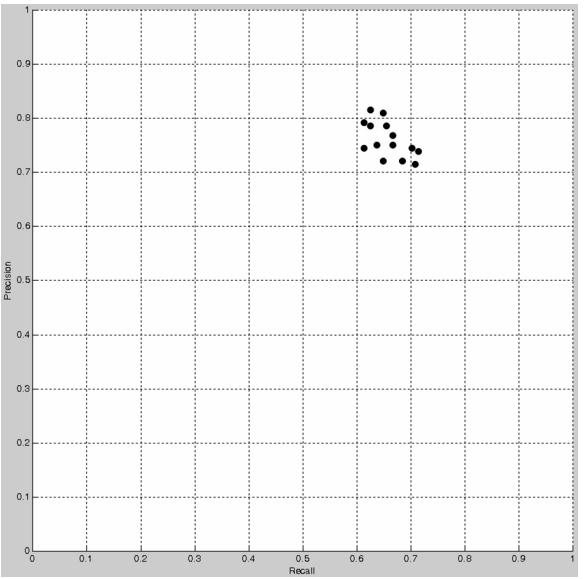

Figure 5: Precision of Navee method in term of F-measure

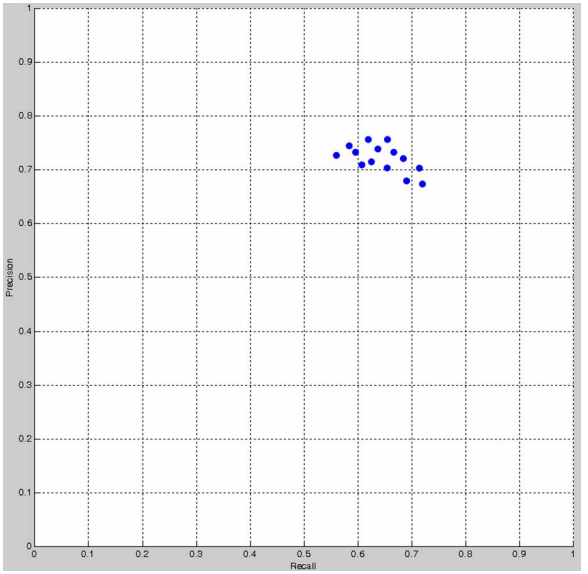

Figure 6: Precision of Khiyati method in term of F-measure

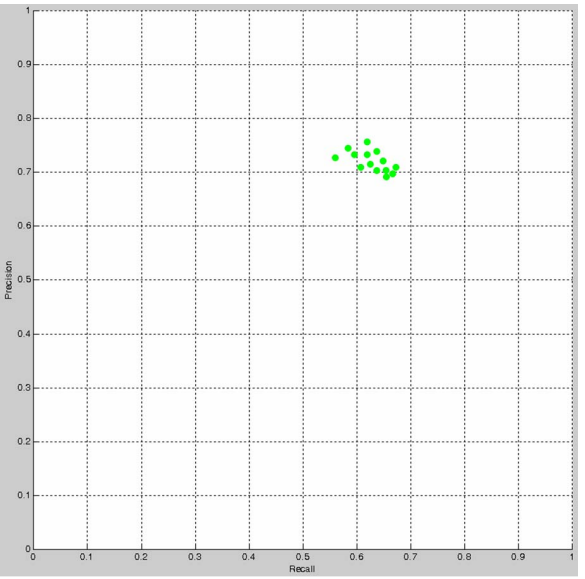

Figure 7: Precision of Van lempt method in term of F-measure

This preprocessing enables us to make use of all dynamic range of 256 levels, and also immune the images from the variation in their intensity. The pixel size was 1mm2, and the slice thickness was 3mm without any gap. For a better evaluation of the proposed method, we investigated supratentorial FLAIR slices, 20 slices per patient in average. The selection of slices was based on presence of lesions, with clear boarders, which enable careful outlining in manual segmentation by our colleagues, a neurologist and a radiologist. At least five slices from each of four patients (at least 20 slices), and 12 slices (in average) from each of the rest, 14 patients, were selected. Thus, totally 217 slices were used. We see that the proposed method is the most ability to detect MS and has the best F-measure score. For each descriptor we reach the best score for method when Dirichlet prior is integrated.

6 Conclusion

We have presented segmentation method based statistical based appearance priors for brain MS segmentation. Existing region-based segmentation methods based on texture features are not suited for MS segmentation as they are not discriminative enough when the appearance of MS and normal tissue overlap. Using priors on the brain/MS appearance calculated on a set of clustered features extracted from the MRI images, we are able to disambiguate the MS lesion from the brain tissue.
We have shown a novel high performance method for the segmentation of MS lesions. One of the main features of this scheme is that it can segment different structures with the same intensity level range. Our scheme also shows some advantages with respect to automatic methods, because it is fairly stable for the segmentation of MS lesion and no image-atlas registration is needed, which is usually a performance bottleneck in other methods. On the other hand, the whole execution time is to be increased around one more minute in order take into account the user interaction to train the classifier. The algorithm shows a high accuracy, depending essentially on the training data-set selected by a medical expert, and it performs really well using multichannel intensity compared to segmentations carried out with only one channel, which is a clear advantage for clinical applications. It is useful for interactive segmentation due to its high performance and the facility to add or remove training prototypes to improve the results. The applications of this method go well beyond MS segmentation since it can be used to segment almost every type of image modalities.

References

Admiraal-Behloul, F.; van den Heuvel, D.; Olofsen, H.; van Osch, M.; der Grond, J.; van Buchem, M.; Reiber (2005): Fully automatic segmentation of

white matter hyperintensities in mr images of the elderly. *J. NeuroImage*, vol. 28, no. 3, pp. 607–617.

Ait-Ali, L.; Prima, S.; Hellier, P.; Carsin, B.; Edan, G.; Barillot, C. (2005): STREM: a robust multidimensional parametric method to segment MS lesions in MRI. In *International Conference on Medical Image Computing and Computer-Assisted Intervention*, volume 3749 of *Lecture Notes in Computer Science*, pp. 409–416. Springer Berlin / Heidelberg.

Anbeek, P.; Vincken, K. L.; van Osch, M. J. P.; Bisschops, R. H. C.; van der Grond, J. (2004): Probabilistic segmentation of white matter lesions in MR imaging. *J. NeuroImage*, vol. 21, no. 3, pp. 1037–1044.

Bazin, P.-L.; Pham, D. (2008): Homeomorphic brain image segmentation with topological and statistical atlases. *Med. Image Anal.*, vol. 12, pp. 616–625.

Benedict, R.; Bobholz, J. (2007): Multiple sclerosis. *Semin. Neurol*, vol. 27, no. 1, pp. 78–85.

Bouguila, N. (2008): Clustering of count data using generalized dirichlet multinomial distributions. *IEEE Trans. Knowl. Data Eng.*, vol. 20, no. 4, pp. 462–474.

Bouguila, N.; Ziou, D. (2004): Dirichlet-based probability model applied to human skin detection. In *Montreal, Canada May 2004*, pp. 521–524.

Bouguila, N.; Ziou, D. (2006): A hybrid sem algorithm for high-dimensional unsupervised learning using a finite generalized dirichlet mixture. *IEEE Transactions on Image Processing*, vol. 15, no. 9, pp. 2657–2668.

Bouguila, N.; Ziou, D. (2007): High-dimensional unsupervised selection and estimation of a finite generalized dirichlet mixture model based on minimum message length. *IEEE Trans. Pattern Anal. Mach. Intell.*, vol. 29, no. 10, pp. 1716–1731.

Bricq, S.; Collet, C.; Armspach, J. (2008): Lesion detection in 3d brain MRI using trimmed likelihood estimator and probabilistic atlas. In *5th International Symposium on Biomedical Imaging*, pp. 93–96.

Chan, T.; Vese, L. (2001): Active contours without edges. *IEEE Trans. Imag. Processing*, vol. 10, no. 2, pp. 266–277.

Cremers, D.; Schnorr, C.; Weickert, J. (2001): Diffusion-snakes : combining statistical shape knowledge and image information in a variational framework. In *IEEE Workshop on Variational, Geometric and Level Set Methods in Computer Vision*, pp. 137–144.

D. Martin, C. Fowlkes, J. M. (2004): Learning to detect natural image boundaries using local brightness, color, and texture cues. *IEEE Trans. PAMI*, vol. 26, no. 5, pp. 530–549.

Derraz, F.; Beladgham, M.; Khelif, M. (2004): Application of active contour models in medical image segmentation. In *ITCC 04: Proceedings of the International Conference on Information Technology: Coding and Computing (ITCC'04) Volume 2*, pp. 675–681, Washington, DC, USA. IEEE Computer Society.

Filippi, M.; H. van Waesberghe, J.; A. Horsfield, M.; Bressi, S.; Gasperini, C.; A. Yousry, T.; L. Gawne-Cain, M.; Morrissey, S. P.; A. Rocca, M.; Barkhof, F.; J. Lycklama-Nijeholt, G.; Bastianello, S.; H. Miller, D. (1997): Interscanner variation in brain MRI lesion load measurements in MS: implications for clinical trials. *Neurology*, vol. 49, no. 2, pp. 371–7.

Filippi, M.; Horsfield, A.; Ader, H. (1998): Guidelines for using quantitative measures of brain magnetic resonance imaging abnormalities in monitoring the treatment of multiple sclerosis. *Ann. Neuro.*, vol. 43, pp. 499–506.

Freifeld, O.; Greenspan, H.; Goldberger, J. (2009): Multiple sclerosis lesion detection using constrained gmm and curve evolution. *Int. J. Biomed. Imaging*, vol. 26, no. 12, pp. 1–13.

GarciaLorenzo, D.; Prima, S.; Collins, D.and Arnold, D.; Morrissey, S.; Barillot, C. (2008): Combining robust expectation maximization and mean shift algorithms for multiple sclerosis brain segmentation. In *Workshop on Medical Image Analysis on Multiple Sclerosis*, pp. 82–91.

Gonalves, P. C.; Tavares, J. M. R.; Jorge, R. N. (2008): Segmentation and simulation of objects represented in images using physical principles. *Computer Modeling in Engineering - Sciences*, vol. 32, no. 2, pp. 45–55.

Grossman, R.; Mcgowan, J. (1998): Perspectives on multiple sclerosis. *AJNR*, vol. 19, pp. 1251–1265.

Harmouche, R.; Collins, L.; Arnold, D.; Francis, S.; Arbel, T. (2006): Bayesian MS lesion classification modeling regional and local spatial information. In *International Conference on Pattern Recognition*, pp. 984–987.

He, L.; Peng, Z.; Everding, B.; Wang, X.; Han, C.; Weiss, K.; Wee, W. (2008): A comparative study of deformable contour methods on medical image segmentation. *Image and Vision Computing*, vol. 26, pp. 141–163.

Johnston, B.; Atkins, M.; Mackiewich, B.; Anderson, M. (1996): Segmentation of multiple sclerosis lesions in intensity corrected multispectral mri. *IEEE Trans. Med. Imag.*, vol. 15, pp. 154–169.

Kamber, M.; Shinghal, R.; Collins, D.; Francis, G.; Evans, A. (1995): Model-based 3-d segmentation of multiple sclerosis lesions in magnetic resonance brain images. *IEEE Trans. Med. Imag.*, vol. 14, pp. 442–453.

Khayati, R.; Vafadust, M.; Towhidkhah, F.; Nabav, S. (2008): A novel method for automatic determination of different stages of multiple sclerosis lesions in brain mr flair images. *Computerized Med.l Imag. and Graphics*, vol. 32, pp. 124–133.

Kim, J.; III, J. W. F.; Yezzi, A. J.; Çetin, M.; Willsky, A. S. (2005): A non-parametric statistical method for image segmentation using information theory and curve evolution. *IEEE Transactions on Image Processing*, vol. 14, no. 10, pp. 1486–1502.

Kurihara, K.; Welling, M.; Teh, Y. W. (2007): Collapsed variational dirichlet process mixture models. In *IJCAI*, pp. 2796–2801.

Kurihara, K.; Welling, M.; Vlassis, N. A. (2006): Accelerated variational dirichlet process mixtures. In *NIPS*, pp. 761–768.

Ma, Z.; Tavares, J. M. R. S.; Jorge, R. N.; Mascarenhas, T. (2010): A review of algorithms for medical image segmentation and their applications to the female pelvic cavity. *Computer Methods in Biomechanics and Biomedical Engineering*, vol. 13, no. 2, pp. 235–246.

Miller, D. (2002): MRI monitoring of MS in clinical trials. *Clinical Neurology and Neurosurgery*, vol. 104, no. 3, pp. 236–243.

Nett, J. (2001): The study of ms using mri image processing and visualization. M. eng. thesis, University of Louisville, 2001.

O. Michailovich, Y. R.; Tannenbaum, A. (2007): Image segmentation using active contours driven by the bhattacharyya gradient flow. *IEEE Trans. Imag. Processing*, vol. 16, no. 11, pp. 2787–2801.

Rauber, T. W.; Braun, T.; Berns, K. (2008): Probabilistic distance measures of the dirichlet and beta distributions. *Pattern Recogn.*, vol. 41, no. 2, pp. 637–645.

S. Jehan-Besson, M. Barlaud, e. G. A. (2003): DREAM2S : deformable regions driven by an eulerian accurate minimization method for image and video segmentation. *International Journal of Computer Vision*, vol. 53, pp. 45–70.

Shiee, N.; Bazin, P.-L.; Ozturk, A.; Reich, D. S.; Calabresi, P. A.; Pham, D. L. (2010): A topology-preserving approach to the segmentation of brain images with multiple sclerosis lesions. *NeuroImage*, vol. 49, no. 2, pp. 1524 –1535.

Souplet, J.; Lebrun, C.; Chanalet, S.; Ayache, N.and Malandain, G. (2008): Approaches to segment multiple-sclerosis lesions on conventional brain mri. *Rev. Neurol.*, vol. 165, no. 1, pp. 7–14.

Van Leemput, K.; Maes, F.; V, Dirk, V.; Colchester, A.; Suetens, P. (2001): Automated segmentation of multiple sclerosis lesions by model outlier detection. *IEEE Trans. on Medical Imaging*, vol. 20, no. 8, pp. 677–688.

Vasconcelos, M. J. M.; Tavares, J. M. R. S. (2008): Methods to automatically built point distribution models for objects like hand palms and faces represented in images. *Computer Modeling in Engineering - Sciences*, vol. 36, no. 3, pp. 213–241.

Warfield, S.; Dengler, J.; Zaers, J.; Guttmann, C. R. G.; Wells, W. M. I.; Ettinger, G.; Hiller, J.; Kikinis, R. (1995): Automatic identification of grey matter structures from MRI to improve the segmentation ofwhitematter lesions. *J Image Guid Surg*, vol. 1, no. 6, pp. 326–338.

Wells, III, W. M.; Grimson, W. E. L.; Kikinis, R.; Jolesz, F. A. (1996): Adaptive segmentation of MRI data. *IEEE Trans. Med. Imag.*, vol. 15, pp. 429–442.

Wu, Y.; Warfield, S.; Tan, I.; Wells, W.; Meier, D.; van Schijndel, R.; Barkhof, F.; Guttmann, C. (2006): Automated segmentation of multiple sclerosis lesion subtypes with multichannel MRI. *J. Neuroimage*, vol. 32, pp. 1205–1215.

Zijdenbos, A.; Dawant, B.; Margolin, R.; Palmer, A. (2000): Morphometric analysis of white matter lesions in mr images method and validation. *IEEE Trans. Med. Imag.*, vol. 13, pp. 716–724.

Zijdenbos, A.; Forghani, R.; Evans, A. (2000): Automatic pipeline analysis of 3-d mri data for clinical trials: application to multiple sclerosis. *IEEE Trans. Med. Imag.*, vol. 21, pp. 1280–1291.

CMES: Computer Modeling in Engineering & Sciences

ISSN : 1526-1492 (Print); 1526-1506 (Online)

Journal website:
http://www.techscience.com/cmes/

Manuscript submission
http://submission.techscience.com

Published by
Tech Science Press
5805 State Bridge Rd, Suite G108
Duluth, GA 30097-8220, USA

Phone (+1) 678-392-3292
Fax (+1) 678-922-2259
Email: sale@techscience.com
Website: http://www.techscience.com
Subscription: http://order.techscience.com

CMES is Indexed & Abstracted in
Applied Mechanics Reviews; Cambridge Scientific Abstracts (Aerospace and High Technology; Materials Sciences & Engineering; and Computer & Information Systems Abstracts Database); CompuMath Citation Index; Current Contents: Engineering, Computing & Technology; Engineering Index (Compendex); INSPEC Databases; Mathematical Reviews; MathSci Net; Mechanics; Science Alert; Science Citation Index; Science Navigator; Zentralblatt fur Mathematik.